

A unified framework and an alternative mechanism for allosteric regulation

Jianhua Xing^{1, 2, 3}

**¹ Chemistry, Material and Life Sciences Directorate, University of California & Lawrence
Livermore National Laboratory, Livermore, CA 94550**

**² Department of Biological Sciences, Virginia Polytechnic Institute and State University,
Blacksburg, VA, 24061-0406**

³ Corresponding email address: jxing@vt.edu

Total characters: 26300; Figures: 4; Pages: 18; Table: 1

Classification: BIOLOGICAL SCIENCES (Biophysics)

Abstract

Allosteric regulation is an important property for many proteins. Several models have been proposed to explain the allosteric effect, such as the concerted MWC (Monod, Wyman, Changeux) model, the sequential KNF (Koshland, Nemethy, Filmer) model, and recent population shift models. Here we discuss a unified theoretical framework to describe allosteric effects. The existing models appear as special cases of the framework. The theoretical work also reveals an alternative mechanism currently overlooked. Theoretically it is possible that the reactivity of a protein is limited by some internal conformational change step (due to slow effective diffusion along rugged potential surfaces). Effector binding may modify the ruggedness and thus the protein dynamics and reactivity. Compared to conventional models, the new mechanism imposes fewer prerequisites on the mechanical properties of an allosteric protein needed to propagate mechanical signals over long distances. For a positive (negative) allosteric enzyme functioning under the new mechanism, the theory predicts that an enzyme in an unbound state compared to its effector bound state has: 1) stronger (weaker) temperature dependence; 2) larger (weaker) effect of dynamic disorder (such as nonexponential waiting time distribution of the turnover cycle); 3) smaller (larger) collective and individual dynamic fluctuations. Moreover, the proposed mechanism does not require a well-defined mechanical strain relaying network, nor does it require large conformational change upon effector binding.

Introduction

A prominent property of proteins is that their catalytic activities can be regulated. Allosteric enzymes have two or more binding sites. Conformational changes due to ligand (effector) binding or reaction on one site can propagate to another distant catalytic site and affect its reactivity. The discovery of allosteric regulations “in the 1950s, followed by a general description of allostery in the early 1960s, was revolutionary at the time”(1). Not surprisingly understanding the allosteric mechanism(s) is an important topic in structural biology. There are two popular models proposed to explain the allosteric effects. The concerted MWC model by Monod, Wyman, and Changeux, assumes that an allosteric protein can exist in two (or more) conformations with different reactivity, and effector binding modifies the thermal equilibrium distribution of the conformers(2). Recent population shift models re-emphasize the idea of preexisting populations (3-9). The sequential model described by Koshland, Nemethy, and Filmer is based on the induced-fit mechanism, and assumes that effector binding results in (slight) structural change at another site and affects the substrate affinity(10). While different in details, both of the above models assume that the allosteric mechanism is through modification of the equilibrium conformation of the allosteric protein by effector binding. For later discussions, we characterize such mechanisms as being driven by “thermodynamic regulation”. The above two mechanisms and generalizations have been used to explain various observed allosteric effects. For example, the allosteric effect is used to explain the working mechanisms of protein motors(11).

The mechanisms of thermodynamic regulation impose strong requirements on the mechanical properties of an allosteric protein. The distance between the two binding sites of an allosteric protein can be far. For example, the bacterial chemotaxis receptor has the two reaction regions separated as far as 15 nm(12). Signal propagation requires a network of mechanical strain relaying residues with mechanical properties distinguishing them from its surroundings to minimize thermal dissipation. Mechanical stresses due to effector molecule binding radiate from the binding site, propagate through the relaying network, and then converge on the reaction region at the other side of the protein. This presents formidable structural challenges to the transmission of mechanical energy against thermal dissipation over a long distance. A possible solution is the attraction shift model proposed by Yu and Koshland(13).

In this work, we will first discuss a unified theoretical framework describing allosteric regulation, from which we will propose an alternative mechanism of allosteric regulation, “kinetic regulation.” In this new scheme, protein reactivity is modulated by modifying protein dynamics, rather than through the influence of large conformational changes and thermodynamic properties such as substrate binding affinity. This idea is inspired by experimental and theoretical studies on dynamic disorder. Dynamic disorder refers to the phenomena that the ‘rate constant’ of a process is actually a statistical function of time, and is affected by slow protein conformational motions (14, 15). Since the pioneering work of Frauenfelder and coworkers on ligand binding to myoglobin(16), extensive experimental and theoretical studies have been performed on this subject (see ref.(15) for further reference). Recently existence of dynamic disorder has been demonstrated directly through single molecule enzymology measurements(17-19).

Theoretical formalism of the allosteric effect

We will first focus on the catalytic site being regulated. The catalytic site can be described by a few slow conformational modes and the reaction coordinates. Here we will use a specific example shown in Figure 1a to illustrate the general idea. The chemical reaction we consider is a head-on group-transfer reaction, $AC + B \rightarrow A + BC$. A possible choice of the reaction coordinate will be $r = R_{AC}/R_{AB}$, the ratio between two distances. The distance R_{AB} is related to some motion along a conformational coordinate. For each of the two conformers in Figure 1a, dynamics along the reaction coordinate is described by a barrier crossing process, as shown in Figure 1b. Conformer 1 has a lower barrier than conformer 2, and thus has higher reactivity. A more complete description is to use the two-dimensional potential surfaces plotted in Figure 1c and d. Current existing models on allosteric effects differ in some details in the potential shapes. The KNF model (exemplified by Figure 1c) emphasizes that without the effector, the protein exists mainly in one form (conformer 2 in our case). Effector binding shifts the protein to another form with different reactivity. The MWC (exemplified by Figure 1d) and the recent population-shift model emphasize that there are pre-existing populations for all the possible forms, and effector binding only shifts their relative populations. The potentials shown in Figure 1c and d are only for illustrative purposes. For example, a protein governed by the KNF mechanism may have double-well shaped potentials as well. For barrier crossing processes, a system spends most of the time near the minimum of the potential wells, and the actual barrier-crossing time is transient. Therefore, one can reduce the two-dimensional surfaces (Figure 1c and d) to one-dimensional projections along the conformational coordinate (Figure 1e), and approximate transitions along the

reaction coordinate by rate processes between the one-dimensional potential surfaces. This representation is widely used to model protein motors(20). Similar idea can also be found in the treatment of allosteric effects by Miyashita et al.(21)

With the above introduction of potential surfaces, we can now formulate a general theoretical framework for allosteric effects. Protein dynamics is affected by substrate binding. Therefore, a minimal model representing the states of a catalytic site is: Emp (empty), Rec (reactant bound), Prod (product bound). Figure 2 illustrates an example used in this work. Each state is described by a potential curve along the conformational coordinate, and localized transitions can occur between two potentials. For an enzymatic cycle, a reactant molecule first binds onto the catalytic site (Emp→Rec), then forms a more compact complex from which a chemical reaction takes place (Rec→Prod), and finally the product is released (Prod→Emp). In the more familiar discrete kinetic form, the overall process can be represented as $E + R \rightleftharpoons ER \rightleftharpoons ER^* \rightleftharpoons EP \rightleftharpoons E + P$, with E, R and P refer to the enzyme, reactant, and product respectively. Notice that in general, locations of the potential minima for different states may not be the same, and some conformational motion is necessary during the cycle. Figure 2b illustrates a system zigzagging downward along the potential surface and its resulting interplay between chemical transitions and conformational movement. The figure resembles that used to describe protein motors(22).

Dynamics of the reduced system can be described by a set of over-damped Langevin equations coupled to Markov chemical transitions (23),

$$\zeta_i \frac{dx(\tau)}{d\tau} = -\frac{dU_i}{dx} + f_i(t), \quad (1)$$

where x represents the conformational coordinate, U_i is the potential of mean force with a given substrate binding state, ζ_i is the drag coefficient, and f is the random fluctuation force with the property $\langle f(t)f(t') \rangle = 2k_B T \zeta \delta(t-t')$, with k_B the Boltamann's constant, T the temperature. Chemical transitions accompany motions along the conformational coordinate with x -dependent transition rates. The dynamics can be equally described by a set of coupled Fokker-Planck equations (here we only consider the steady state),

$$-\frac{D_i}{k_B T} \cdot \frac{\partial}{\partial x} \left(-\frac{\partial U_i(x)}{\partial x} \rho_i \right) + D_i \frac{\partial^2 \rho_i}{\partial x^2} + \sum_{j \neq i} (K_{ij}(x) \rho_j - K_{ji}(x) \rho_i) = 0, (2)$$

Where $D_i = k_B T / \zeta_i$ is the diffusion constant, K_{ij} is the transition matrix element, and ρ_i is the probability density to find the system at position x and state i .

Current existing models assume that effector binding at a remote site can affect the dynamics at the catalytic site by modifying U_i . While differing in details, these models assume that a quasi-equilibrium distribution can be established along the conformational coordinate, and therefore, a thermodynamic treatment is appropriate. These models describe a “thermodynamic regulation” mechanism. However, the quasi-equilibrium approximation can break down, and the drag coefficient ζ_i , can also be regulated, which leads to a “kinetic regulation mechanism” discussed below.

Kinetic regulation mechanism

The kinetic regulation mechanism is based on the experimental observation that protein conformational fluctuations can be very slow (e.g. from milliseconds to hundred seconds (19)(9)). Therefore, the equilibrium assumption in the existing allosteric effect models may not be valid. Variation of the dynamic properties along the conformational coordinate can have a dramatic effect on the apparent protein reactivity. Our recent theoretical analysis showed that the observed slow protein conformational dynamics can be explained by rugged protein potential surfaces(24). As one source of the ruggedness, irregular shapes of protein surfaces result in frequent random collisions during relative motions between different protein parts (see Figure 3b). The relative motions are then characterized by hopping over numerous potential barriers (refer to inlet of Figure 2a). For a potential surface with random ruggedness, Zwanzig showed that the barrier-hopping process can be approximated by diffusion along a coarse-grained smooth potential with an effective diffusion constant $D = D_0 \exp\left(-(\varepsilon / k_B T)^2\right)$, where D_0 is the bare diffusion constant, and ε is the potential roughness parameter(25). The reported value of ε is 2-6 $k_B T$ (26, 27). With $D_0 = 10^{-6} \text{ cm}^2/\text{s}$, D can be reduced to $1 \text{ \AA}^2/\text{s}$ with $\varepsilon \sim 4.8 k_B T$. Thus internal diffusion can be a rate limiting step for enzymatic reactions and in principle can be regulated by allosteric effects (see Figure 2).

Kinetic regulation mechanism as an alternative model for allosteric effect

In addition to being a theoretical possibility, the dynamic regulation mechanism also has the following improvements over the conventional thermodynamic regulation mechanisms.

First, it is an effective way to regulate the reactivity at a distant region. To increase the reactivity by 10^{10} through an Arrhenius process, the activation barrier needs to be lowered by $23 k_B T$. On the other hand, for an internal diffusion limited process, the reaction rate is linearly dependent on the effective diffusion constant. To increase the reactivity by the same 10^{10} , the lower bound of the roughness parameter only needs to be adjusted by $\sim 5 k_B T$.

Secondly, the kinetic regulation mechanism has less requirements on the mechanical properties of the protein. Figure 1e schematically shows the free energy profiles of a protein with and without the effector under the conventional allosteric mechanism. The free energy difference between the two curves, $\Delta U(x)$, can be derived from the effector binding energy as a function of the conformational coordinate. Effective coupling of the two sites requires a faithful finely tuned transmission of the mechanical strain due to ligand binding from one site to another one. In terms of solid mechanics, the mechanical stress lines should propagate from one site and locally converge on another site. A set of mechanical stress relaying network is expected to perform the task(28). As illustrated in Figure 3a, these network residues must have mechanical properties distinctive from other residues to minimize energy dissipation to the surroundings. Otherwise, a significant portion of the effector binding energy would be wasted. In other words, coupling between

these relaying residues and others should be minimized. By comparison, under a dynamics regulation mechanism, the effect of effector binding can be highly nonlocal. As illustrated in Figure 3b, effector binding may affect the other site by finely regulating local structures far away from that site. By modifying the effective diffusion constant, these local modifications may affect the dynamics along the conformational coordinate x in our formalism. The latter is usually composed of collective motions of residues within the catalytic site and those far from it. The effect manifests itself through larger root-mean-square deviation as observed in NMR, x-ray crystallography, and in molecular dynamics simulations(5)(9)(6). The dynamics of the collective motions should be examined as well.

Theoretical predictions

In our numerical calculations, the potentials are chosen to be harmonic potentials,

$$V_i = \frac{1}{2} \kappa_i (x - x_{0i})^2 + V_{0i}, \quad i = (\text{Emp}, \text{Rec}, \text{Prod}).$$

To model transitions between different

states, we also model the transition state potentials by harmonic potentials,

$$V_{ij}^\dagger = \frac{1}{2} \left((x - x_{ij}^c) / L_{ij} \right)^2 + V_{ij}^\dagger.$$

The transition rate from state j to i is given by

$$k_{ij}(x) = k_{ij}^0 \exp \left[\left(V_j(x) - V_{ij}^\dagger(x) \right) / k_B T \right].$$

In general the optimal transition location is different for different reactions, and some conformational motion is needed during an enzymatic cycle. Model parameters are given in Table 1.

The Fokker-Planck equations were solved using an algorithm developed by Wang *et al*(29). Figure 4a shows the calculated enzyme turnover rate as a function of the internal diffusion constant. While the diffusion constant is not a rate-limiting parameter at high

values (as compared to the chemical transition rates), at smaller values of D the turnover rate depends on the diffusion constant linearly which is a signature for the existence of diffusion-limited steps. Figure 4b shows the temperature dependence of the turnover rate. With high values of D , the exponential $1/T$ dependence mainly comes from the Arrhenius dependence of the transition rates. However with small values of D , the turnover rate shows strong non-exponential dependence, since the effective diffusion constant D has a Gaussian dependence on $1/T$. Therefore the theory predicts strong non-exponential temperature dependence of enzyme activity in the absence of the effector provided it is regulated by the kinetic mechanism. Figure 4c also shows the waiting time distribution between two consecutive turnover cycles. The results are calculated using the formula first derived by Gopich and Szabo (30). A system with low D values shows non-exponential distribution due to dynamic disorder. At high D values, effects of the dynamic disorder diminish and the distribution is exponential. Therefore, we predict that an enzyme functioning under the kinetic regulation mechanism shows larger dynamic disorder effects. This can be directly tested by measuring consecutive single enzyme turnover time distributions with and without the effector, an extension of the work done by the Xie group(18).

In the current study, we use the Langevin equations to describe motion along the conformational coordinate. In general the dynamics should be described by a set of over-damped generalized Langevin equations coupled to Markov chemical transitions (23),

$$0 = -\frac{dU_i}{dx} - \zeta_i \int_0^t d\tau M_i(t-\tau) \frac{dx(\tau)}{d\tau} + f_i(t), (3)$$

The memory kernel M describes how the dynamics along the x coordinate is affected by the dynamics of the remaining implicit degrees of freedom at earlier time. Theoretically M can also be regulated, although many studies suggest a universal power-law form(19). We also performed numerical simulations of the coupled generalized Langevin equations have power-law memory kernels. The results also demonstrate that enzyme reactivities can be regulated by modifying ζ , consistent with the Langevin dynamics results.

Concluding remarks

In this work we propose a unified theoretical framework describing allosteric regulation, with existing models as special cases. Inspired by recent experimental studies on dynamic disorder, we also propose a kinetic regulation mechanism. We suggest that protein dynamics can be rate-limited by some internal diffusion steps, and effector binding can change the protein reactivity by accelerating the diffusion step. The allosteric mechanism of a given protein has contribution from both thermodynamic regulation (the conventional conformational change mechanism and the newly proposed entropic effect), and dynamic regulation proposed in this work (see also Equation (1)). Different proteins may differ on which effect is dominant.

Recent work relating protein dynamic properties with allosteric effects have been extensively studied by both experimental and simulation techniques (3, 5-7, 9, 12, 31-36). It is proposed that the entropic changes associated with ligand binding contribute to the allosteric effect. This mechanism still falls into the category of “thermodynamic regulation” discussed in this paper, since its effect is to modify the free energy function $U(x)$. The kinetic mechanism discussed in this work is related (since both kinetic and

thermodynamic descriptions consider the effect of rugged free energy landscapes(37)) but differs in whether conformational motion is sufficiently slow to affect the protein reactivity. Some of the experimental evidence in support of a dynamic entropic effect, may also be explained by the kinetic mechanism discussed in this work. For example, both suggest a distribution of protein conformations, and minimize the need for a well-defined mechanical strain relaying network to describe the mechanism of allosteric effects. In addition, slow conformational dynamics has been observed for allosteric proteins(9) further supporting the validity of our formalism.

Acknowledgements

Drs. Daniel Barsky and Ken Kim at LLNL read through the manuscript and provided many helpful comments. JX is supported by a Lawrence Livermore National Laboratory Directed Research and Development grant, and by a Chemistry, Material, and Life Sciences Directorate fellowship. This work was performed under the auspices of the U.S. Department of Energy by the University of California, Lawrence Livermore National Laboratory under Contract No. W-7405-Eng-48.

References

1. Alberts, B., Johnson, A., Lewis, J., Raff, M., Roberts, K. & Walter, P. (2002) *Molecular Biology of the Cell* (Garland, New York).
2. Monod, J., Wyman, J. & Changeux, J. P. (1965) *J. Mol. Biol.* **12**, 88-&.
3. Eisenmesser, E. Z., Bosco, D. A., Akke, M. & Kern, D. (2002) *Science* **295**, 1520-1523.
4. Eisenmesser, E. Z., Bosco, D. A., Akke, M. & Kern, D. (2002) *Biophys. J.* **82**, 137a-137a.
5. Kern, D. & Zuiderweg, E. R. P. (2003) *Curr. Opin. Struc. Biol.* **13**, 748-757.
6. Formanek, M. S., Ma, L. & Cui, Q. (2006) *Proteins-Structure Function and Bioinformatics* **63**, 846-867.
7. Pan, H., Lee, J. C. & Hilser, V. J. (2000) *Proc. Natl. Acad. Sci. U.S.A.* **97**, 12020-12025.
8. Ming, D. & Wall, M. E. (2005) *Phys. Rev. Lett.* **95**, -.
9. Volkman, B. F., Lipson, D., Wemmer, D. E. & Kern, D. (2001) *Science* **291**, 2429-2433.
10. Koshland, D. E., Nemethy, G. & Filmer, D. (1966) *Biochemistry* **5**, 365-&.
11. Xing, J., Liao, J.-C. & Oster, G. (2005) *Proc. Natl. Acad. Sci. USA* **102**, 16539-16546.
12. Kim, S. H., Wang, W. R. & Kim, K. K. (2002) *Proc. Natl. Acad. Sci. U.S.A.* **99**, 11611-11615.
13. Yu, E. W. & Koshland, D. E. (2001) *Proc. Natl. Acad. Sci. U.S.A.* **98**, 9517-9520.
14. Frauenfelder, H., Wolynes, P. G. & Austin, R. H. (1999) *Rev. Mod. Phys.* **71**, S419-S430.
15. Zwanzig, R. (1990) *Acc. Chem. Res.* **23**, 148-152.
16. Austin, R. H., Beeson, K. W., Eisenstein, L., Frauenfelder, H. & Gunsalus, I. C. (1975) *Biochemistry* **14**, 5355-5373.
17. Xie, X. S. & Lu, H. P. (1999) *J. Biol. Chem.* **274**, 15967-15970.
18. English, B. P., Min, W., van Oijen, A. M., Lee, K. T., Luo, G. B., Sun, H. Y., Cherayil, B. J., Kou, S. C. & Xie, X. S. (2006) *Nat. Chem. Biol.* **2**, 87-94.
19. Min, W., Luo, G. B., Cherayil, B. J., Kou, S. C. & Xie, X. S. (2005) *Phys. Rev. Lett.* **94**, 198302-.
20. Xing, J., Wang, H.-Y. & Oster, G. (2005) *Biophys. J.* **89**, 1551-1563.
21. Miyashita, O., Onuchic, J. N. & Wolynes, P. G. (2003) *Proc. Natl. Acad. Sci. U.S.A.* **100**, 12570-12575.
22. Bustamante, C., Keller, D. & Oster, G. (2001) *Acc. Chem. Res.* **34**, 412-420.
23. Zwanzig, R. (2001) *Nonequilibrium Statistical Mechanics* (Oxford University Press, Oxford).

24. Xing, J. & Kim, K. S. (2006) *Phys. Rev. E* **74**, 061911.
25. Zwanzig, R. (1988) *Proc. Natl. Acad. Sci. U.S.A.* **85**, 2029-2030.
26. Nevo, R., Brumfeld, V., Kapon, R., Hinterdorfer, P. & Reich, Z. (2005) *EMBO Rep.* **6**, 482-486.
27. Thirumalai, D. & Woodson, S. A. (1996) *Acc. Chem. Res.* **29**, 433-439.
28. Dima, R. I. & Thirumalai, D. (2006) *Protein Science* **15**, 258-268.
29. Wang, H., Peskin, C. & Elston, T. (2003) *J. Theo. Biol.* **221**, 491-511.
30. Gopich, I. V. & Szabo, A. (2006) *J. Chem. Phys.* **124**, -.
31. Liu, T., Whitten, S. T. & Hilser, V. J. (2006) *Proteins-Structure Function and Bioinformatics* **62**, 728-738.
32. Rueda, D., Bokinsky, G., Rhodes, M. M., Rust, M. J., Zhuang, X. W. & Walter, N. G. (2004) *Proc. Natl. Acad. Sci. U.S.A.* **101**, 10066-10071.
33. Palmer, A. G. (2004) *Chem. Rev.* **104**, 3623-3640.
34. Eisenmesser, E. Z., Millet, O., Labeikovsky, W., Korzhnev, D. M., Wolf-Watz, M., Bosco, D. A., Skalicky, J. J., Kay, L. E. & Kern, D. (2005) *Nature* **438**, 117-121.
35. Fuentes, E. J., Gilmore, S. A., Mauldin, R. V. & Lee, A. L. (2006) *J. Mol. Biol.* **364**, 337-351.
36. Gunasekaran, K., Ma, B. Y. & Nussinov, R. (2004) *Proteins-Structure Function and Bioinformatics* **57**, 433-443.
37. Hilser, V. J., Garcia-Moreno, B., Oas, T. G., Kapp, G. & Whitten, S. T. (2006) *Chem. Rev.* **106**, 1545-1558.

Figure captions

Figure 1 A schematic example to illustrate the formalism. (a) At the catalytic site, group C is transferred from A to B. The catalytic site can have more than one conformation represented by the distance R_{AB} . (b) Corresponding free energy profiles along the reaction coordinate $r = R_{AC}/R_{AB}$. The barrier height is much lower for conformer 1 than for conformer 2. (c) Schematic two-dimensional potential surfaces by including the conformational changes along the coordinate R_{AB} with (left) and without (right) effector. Without effector, the population of conformer 1 is negligible. This example may represent the KNF model. (d) Similar potential surfaces represent the MWC and the population shift models. Both conformer 1 and 2 are populated with and without effector. (e) Corresponding potential profiles projected onto the conformational coordinate. Left is for case (c), and right is for case (d). Red: with effector. Blue: without effector.

Figure 2 A minimal model for the catalytic site. (a) The free energy curves represent three distinct catalytic site binding states (Emp, Rec, Prod) projected onto a conformational coordinate x . Chemical transitions between the three states are centered at some x values. The inset illustrates that the smooth potentials are actually coarse-grained over rugged potential surfaces. Effector binding at a distant site may modify the roughness of the potentials. (b) Portion of the corresponding two-dimensional potentials. Note that in general, the locations of the potential minima are different for different states.

Figure 3 schematic illustrations of different regulation mechanisms. (a) For thermodynamic regulations, effective coupling of the two binding sites require a network of residues to transmit mechanical stress between the two sites in spite of thermal dissipation. These residues are expected to have solid-like properties, and are distinctive from the surrounding residues. (b) For kinetic regulation, effector binding may cause small conformational changes away from the catalytic site.

Figure 4 Theoretical predictions. (a) Enzyme turnover rate as a function of the effective internal diffusion constant D . (b) Temperature dependence of the enzyme turnover rate. $D = D_0 \exp[-(\varepsilon/k_B T)^2]$,

where ε is the roughness parameter, and $D_0 = 10^3$. Solid line: $\varepsilon = 0$. dashed line: $\varepsilon = 4 k_B T$. The temperature dependence of D_0 is neglected in this calculation. (c) Turnover waiting time distribution with $D = 1$ (solid line) and $D = 0.001$ (dashed line).

Table

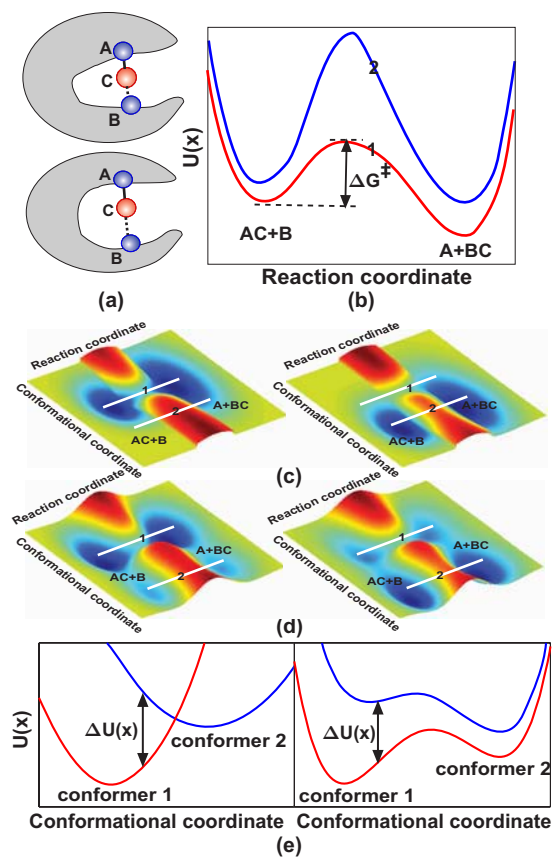
Potential parameters

	κ	x_0	V_0
E	1	1	0
R	0.5	-0.5	-1
P	0.4	0	-3

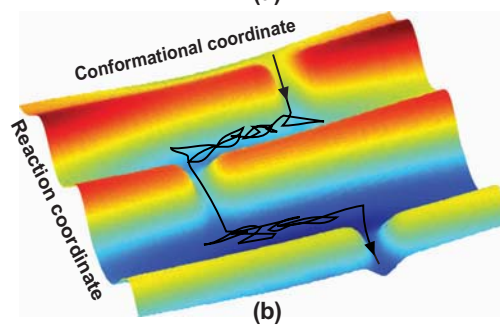
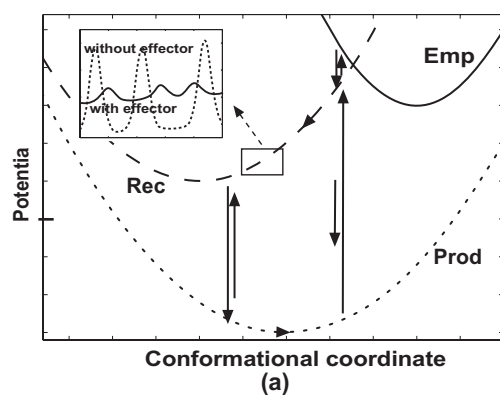
Transition parameters

	R \leftarrow E	P \leftarrow E	E \leftarrow R	P \leftarrow R	E \leftarrow P	R \leftarrow P
k^0	2e2	2e-3	2e2	1.6e3	2e3	1.6e3
V_0^\dagger	3	3	3	6	3	6
L	0.3	0.3	0.3	0.3	0.3	0.3
x_{ij}^c	0.65	0.65	0.65	-0.65	0.65	-0.65

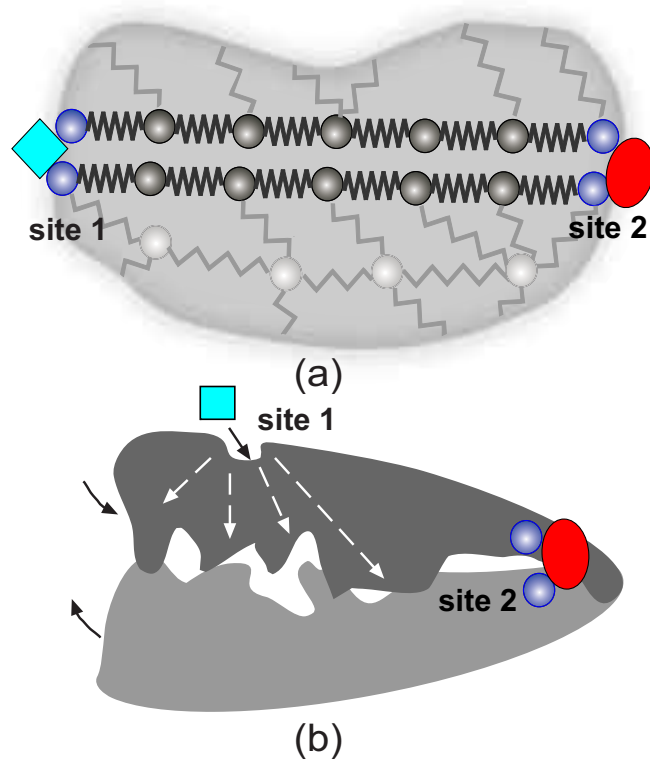
Table 1 Model parameters. Here E, R, and P refer to the three substrate binding states Emp, Rec, and Prod. All energy units in this table are in reduced units: for energy $k_B T = 1$. For simplicity, the diffusion constants for the three states take the same value. The prefactors of the rate constants are chosen so that the maximum values of k_{RE} , k_{PR} , and k_{EP} are approximately 10, 1.5, and 5, respectively.



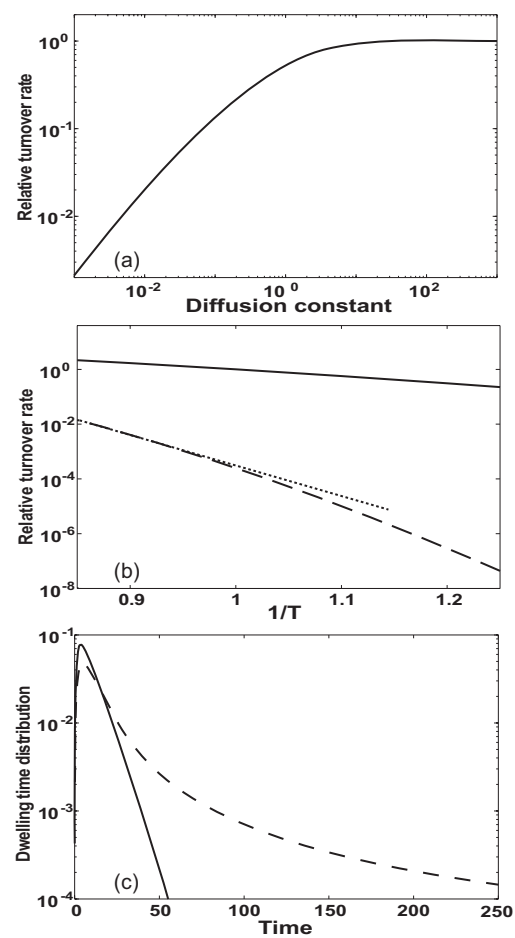
Xing, Figure 1



Xing, Figure 2



Xing, Figure 3



Xing, Figure 4